

Quantum tunneling in a three-dimensional network of exchange-coupled single-molecule magnets

R. Tiron,¹ W. Wernsdorfer,¹ N. Aliaga-Alcalde,² and G. Christou²

¹Laboratoire Louis Néel, associé à l'UJF, CNRS, BP 166, 38042 Grenoble Cedex 9, France

²Department of Chemistry, University of Florida, Gainesville, Florida 32611-7200, USA

(Received 26 June 2003; published 15 October 2003)

A Mn_4 single-molecule magnet is used to show that quantum tunneling of magnetization is not suppressed by moderate three-dimensional exchange coupling between molecules. Instead, it leads to an exchange bias of the quantum resonances which allows precise measurements of the effective exchange coupling that is mainly due to weak intermolecular hydrogen bonds. The magnetization versus applied field was recorded on single crystals of $[\text{Mn}_4]_2$ using an array of micro-superconducting quantum interference devices. The step fine structure was studied via minor hysteresis loops.

DOI: 10.1103/PhysRevB.68.140407

PACS number(s): 75.45.+j, 75.60.Ej, 75.50.Xx

Single-molecule magnets (SMM's), such as Mn_{12} , Mn_4 and Fe_8 ,¹⁻⁵ have become model systems to study quantum tunneling of magnetization (QTM).⁶⁻¹¹ These molecules comprise several magnetic ions, with their spins coupled by strong exchange interactions to give a large effective spin. The molecules are regularly assembled in large crystals where often all the molecules have the same orientation. Hence, macroscopic measurements can give direct access to single-molecule properties. Many nonmagnetic atoms surround the magnetic core of each molecule. Exchange interactions between molecules are therefore relatively weak and have been neglected in most studies.

Recently, the study of a dimerized SMM $[\text{Mn}_4]_2$ showed that intermolecular exchange interactions are not negligible.¹² This compound belongs to the $[\text{Mn}_4\text{O}_3\text{Cl}_4(\text{O}_2\text{CR})_3(\text{py})_3]_2$ family, with $R = \text{CH}_2\text{CH}_3$ and it will be named in the following as compound 1. The spins of the two Mn_4 molecules are coupled antiferromagnetically. Each molecule acts as a bias on its neighbor, the quantum tunneling resonances thus being shifted with respect to the isolated SMM. In this paper we show that even in three-dimensional networks of exchange coupled SMMs, ordering effects do not quench tunneling.

We selected a dimerized SMM $[\text{Mn}_4]_2$, called compound 2. The molecule belongs to the same family as compound 1, however $R = \text{CH}_3$. Because this substituent has a smaller volume than $R = \text{CH}_2\text{CH}_3$, molecules are packed slightly closer together. This leads to stronger interdimer interactions, which are negligible in compound 1. The preparation, x-ray structure, and detailed physical characterization have been reported elsewhere.^{13,14} Compounds 1 and 2 crystallize in the hexagonal space group $R\bar{3}$ (bar) with two Mn_4 molecules per unit cell lying head-to-head on a crystallographic S_6 symmetry axis (Fig. 1). The unit-cell parameters are nearly identical: $a = b = c = 13.156 \text{ \AA}$ and 13.031 \AA , $\alpha = \beta = \gamma = 74.56(3)^\circ$ and $74.81(2)^\circ$, $V = 2.06864 \text{ nm}^3$ and 2.01593 nm^3 , respectively for compound 1 and 2. Each monomer Mn_4 has a ground-state spin $S = 9/2$. The Mn-Mn distances and the Mn-O-Mn angles are similar and the uniaxial anisotropy constant is expected to be the same for the two dimer systems. These dimers are held together via six $\text{C}-\text{H}\cdots\text{Cl}$ hydrogen bonds between the pyridine (py) rings on one molecule and the Cl ions on the other and one

$\text{Cl}\cdots\text{Cl}$ Van der Waals interaction [Fig. 1(a)]. These interactions lead to an antiferromagnetic superexchange interaction between the two Mn_4 units of a dimer.¹²

Owing to the S_6 symmetry of $[\text{Mn}_4]_2$, each Mn_4 is close to three neighboring Mn_4 molecules of the three neighboring $[\text{Mn}_4]_2$ [Fig. 1(b)]. There are hydrogen bonds between the pyridine (py) rings of the molecules and the O ions of the other three neighboring molecules. The $\text{C}-\text{H}\cdots\text{O}$ hydrogen bonds between $[\text{Mn}_4]_2$ dimers have $\text{C}\cdots\text{O}$ distances and $\text{C}-\text{H}\cdots\text{O}$ angles of 4.20 \AA and 124.37° , or 4.05 \AA and 124.85° , respectively for compounds 1 and 2. The interactions between the dimers are expected to be antiferromagnetic and weaker than the intradimer interactions. The two different antiferromagnetic couplings, the stronger one inside the dimer and the weaker one between the dimers, make this system an interesting candidate for studying the QTM in a three-dimensional network of exchange-coupled SMM's.

The magnetization versus applied field was recorded on single crystals of $[\text{Mn}_4]_2$ using an array of micro-superconducting quantum interference devices.¹⁵ Figures 2(a) and 2(b) show typical hysteresis loops of magnetization versus applied field for different field sweep rates and at 40 mK, which is well below the crossover temperature of 0.35 K to the pure quantum regime.¹² The field is applied along the easy axis of magnetization of a single crystal of about $20 \mu\text{m}$. These loops display steplike features separated by plateaus. The hysteresis loops of the two crystals are similar. However, compound 2 shows a fine structure that is absent in the hysteresis loops of compound 1. We will show in the following that the main features of the hysteresis loops can be explained by the QTM of one Mn_4 molecule, coupled by a superexchange interaction J to the other unit of the $[\text{Mn}_4]_2$ dimer. We discuss first compound 1 because the coupling with neighboring dimers can be neglected.¹² Then, we show that the fine structure observed for compound 2 is induced by a superexchange interaction J' between neighboring dimers [Fig. 1(b)].

The simplest Hamiltonian describing the spin system of an isolated SMM is

$$\mathcal{H} = -DS_z^2 + \mathcal{H}_{\text{trans}} + g\mu_B\mu_0\vec{S}\cdot\vec{H}, \quad (1)$$

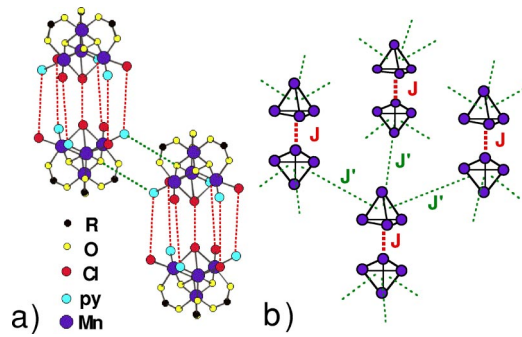


FIG. 1. (Color online) (a) X-ray crystal structure of the Mn₄ dimer. $R = \text{CH}_2\text{CH}_3$ for compound 1 and $R = \text{CH}_3$ for compound 2. The two molecules of a dimer are held together by six hydrogen bonds between the pyridine rings (py) and the Cl ions, and one Cl...Cl van der Waals interaction (3.86 Å and 3.74 Å for 1 and 2, respectively). Two neighboring dimers interact via two hydrogen bonds between the py and the O ion. (b) Schematic view of the exchange-coupled network of Mn₄ molecules. Each Mn₄ molecule (schematized by the Mn₄ tetrahedron) is exchange coupled to the Mn₄ of the dimer (J) and to three molecules of nearby dimers (J').

S_x , S_y , and S_z are the components of the spin operator; D is the anisotropy constant defining an Ising type of anisotropy; $\mathcal{H}_{\text{trans}}$, containing S_x or S_y spin operators, gives the transverse anisotropy which is small compared to DS_z^2 in SMMs; and the last term describes the Zeeman energy associated with an effective field \vec{H} . For one isolated spin the effective field is the applied field. This Hamiltonian has an energy-level spectrum with $(2S+1)$ values which, to a first approximation, can be labeled by the quantum numbers $M = -S, -(S-1), \dots, S$, taking the z axis as the quantization axis. The energy spectrum can be obtained by using standard diagonalization techniques. At $\vec{H} = 0$, the levels $M = \pm S$ have the lowest energy. When a positive field H_z is applied, the levels with $M > 0$ decrease in energy, while those with $M < 0$ increase. Therefore, energy levels of positive and negative quantum numbers cross at certain values of H_z given by $\mu_0 H_z \approx nD/g\mu_B$, where $n = 0, 1, 2, 3, \dots$. When the spin Hamiltonian contains transverse terms $\mathcal{H}_{\text{trans}}$, the level crossings can be *avoided level crossings*.¹¹ The spin S is *in resonance* between two states when the local longitudinal field is close to an avoided level crossing. The energy gap, the so-called *tunnel splitting* Δ , can be tuned by a transverse field (a field applied perpendicular to the z direction) via the $S_x H_x$ and $S_y H_y$ Zeeman terms. The effect of these avoided level crossings leads to well-defined steps in hysteresis loop measurements.

The main point to note is that the giant spin Hamiltonian predicts always the first level crossing at zero field, corresponding to the QTM of a SMM between $M = \pm S$ states. Thus, for compound 1 [see Fig. 2(a)], the single-spin Hamiltonian is not sufficient to explain the first resonance shifted to negative fields and the absence of the quantum tunneling at zero field, in contrast to other SMMs.

In order to explain the observed features in Fig. 2(a), one has to take into account the superexchange coupling J between pairs of Mn₄ units. A Hamiltonian for the two-coupled

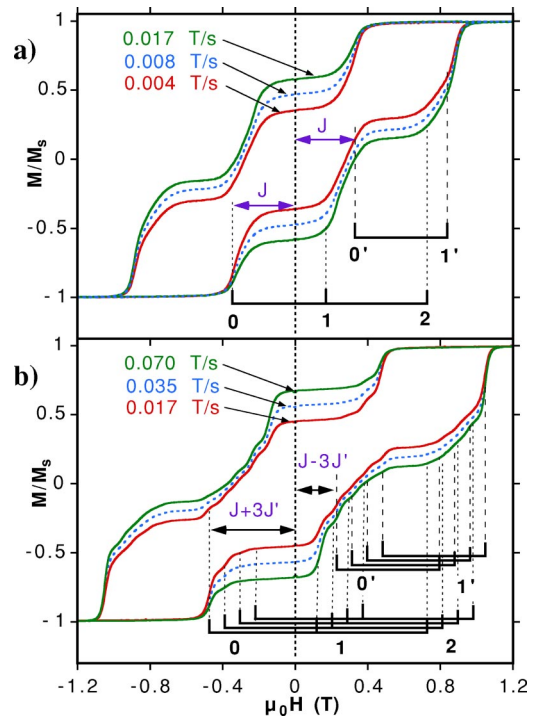


FIG. 2. (Color online) Hysteresis loops for compounds 1 (a) and 2 (b), measured at different sweep rates and at 40 mK. If the spin of one molecule is in the $-9/2$ state, the resonance positions of the other molecule are shifted towards negative fields. The comb (0,1,2) represents the resonances of one molecule from $-9/2$ to $+9/2$ (0), from $-9/2$ to $+7/2$ (1), and from $-9/2$ to $+5/2$ (2). If the spin of the other molecule is in the $+9/2$ states, the resonances are shifted towards positive fields, indicated by the comb ($0'$, $1'$). The step fine structure of compound 2 is explained by exchange coupling with neighbors. It can be explained by the splitting of each comb into four combs (b).

molecules can be written and the energy states of the $[\text{Mn}_4]_2$ can be calculated by exact diagonalization. More details on the dimer Hamiltonian and the corresponding Zeeman diagram are reported elsewhere.¹² Here, we propose a phenomenological model that is sufficiently simple to allow inclusion, in a second step, of more exchange couplings. The influence of the exchange coupling of the neighboring molecule is taken into account by an exchange-bias field H_{bias} . The effective field H_z acting on the molecule is therefore the sum of the applied field H_{app} and the bias field H_{bias} :

$$H_z = H_z^{\text{app}} + H_z^{\text{bias}} = H_z^{\text{app}} + \frac{J}{g\mu_B\mu_0} M_2, \quad (2)$$

where M_2 is the quantum number of the neighboring molecule and J is the associated exchange coupling. In the following we explain the hysteresis loops when the field H_z^{app} is swept from negative to positive values. At low temperature, M_2 has two possible values, $M_2 = \pm S = \pm 9/2$. We therefore expect resonant QTM for applied fields $\mu_0 H_z^{\text{app}} \approx nD/g\mu_B \pm M_2 J/g\mu_B$, where $n = 0, 1, 2, 3, \dots$. The two possibilities of M_2 are represented by two combs in Fig. 2(a). The first comb

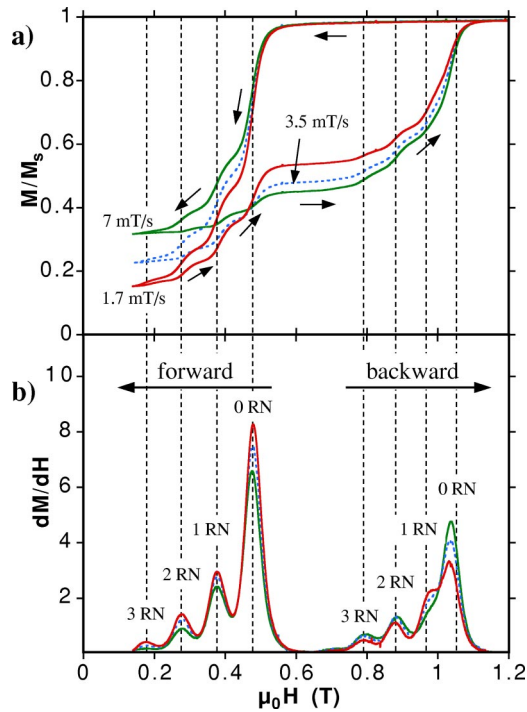


FIG. 3. (Color online) Field sweep rate dependence of (a) the minor hysteresis loops and (b) the derivatives of the hysteresis loops, measured on a single crystal of compound 2 at 0.04 K. The positions corresponding to 0, 1, 2, or 3 reversed neighbors (RN) are indicated.

(0,1,2) corresponds to $M_2 = -9/2$ and the second one (0',1') to $M_2 = 9/2$. This model describes all observed quantum transitions in Fig. 2(a) with two fitting parameters $D/k_B = -0.72$ K and $J/k_B = 0.1$ K. It neglects co-tunneling and other two-body tunnel transitions having a lower probability of occurrence.^{12,16}

Compound 2 displays hysteresis loops [Fig. 2(b)] similar to those of compound 1. However, the total exchange coupling is larger for compound 2. The values of $D/k_B = -0.75$ K and $J/k_B = 0.15$ K were obtained from the field positions of the steps in the hysteresis loops. Another difference between the two compounds is that the hysteresis loops of compound 2 exhibit fine structure that can not be explained by the dimer model described above [Eq. (2)]. In order to better analyze this fine structure, minor hysteresis loops were measured (Figs. 3 and 4). First, the sample is saturated in positive field; all the molecules are in the $M = +9/2$ state. Then the field is decreased. The system approaches the first avoided energy-level crossing at a field value of ≈ 0.5 T. A fraction of the dimers switches from $+9/2$ to $-9/2$, and the total magnetization of the system decreases, generating a step in the hysteresis loop. When the magnetization reaches the second plateau (≈ 0.2 T), the field is swept back towards positive saturation; the tunneling from $M = -9/2$ to $9/2$ is favored via the excited state $7/2$ (≈ 1 T). After this transition the sample reaches positive saturation. The purpose of these minor hysteresis loops is to confirm the fine structure of each transition starting from different initial states.

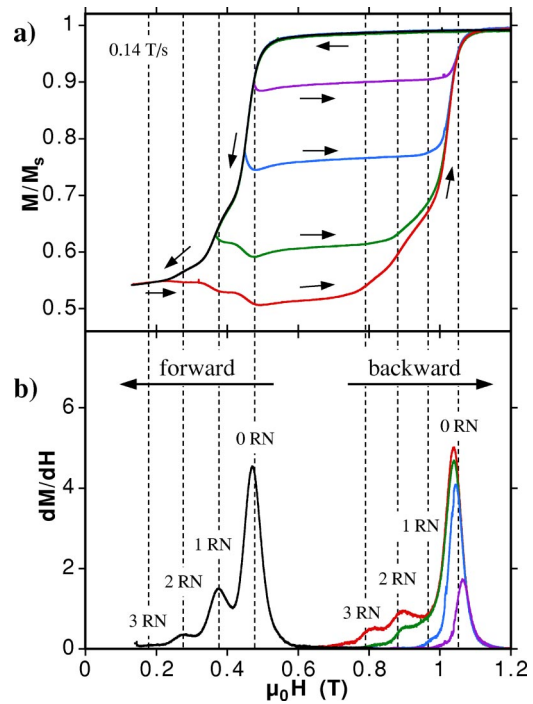


FIG. 4. (Color online) (a) Several minor hysteresis loops and (b) their derivatives, measured on a single crystal of compound 2 at 0.04 K. The field sweep rate is 0.14 T/s. The positions corresponding to 0, 1, 2, or 3 RN are indicated.

The tunnel transitions exhibit four equidistant kinks, which we explain by the exchange coupling to the three neighboring dimers.¹⁷ The spins of the three neighboring molecules can be either aligned with the magnetic field or reversed, leading to four different situations: from zero to three reversed neighbors.

The exchange coupling between a molecule and its neighbors acts like a supplementary field bias and shifts further the resonance fields. The total field bias induced by the neighbors and the other Mn_4 unit of the dimer can be written as

$$H_{\text{bias}}^{\text{tot}} = \frac{1}{g\mu_B\mu_0} \left(JM_2 + \sum_{i=1}^3 J' M'_i \right), \quad (3)$$

where the first term is the contribution of the intradimer coupling, and M'_i is the quantum number of the three neighboring dimer molecules i [Fig. 1(b)].

After positive saturation all the molecules are aligned with the field. The first kink in the hysteresis loop corresponds to the QTM of one molecule in the bias field of its nonreversed neighbors. The resonance is shifted towards negative values by the bias field $H_{\text{bias}} = 9/(2g\mu_B\mu_0)(J + 3J')$ [see Eq. (4)]. After this first kink, some molecules now have one reversed neighbor. At the second kink it is this newly created population which tunnels generating molecules with two reversed neighbors. The corresponding field shift is $H_{\text{bias}} = 9/(2g\mu_B\mu_0)(J + J')$. The third and the fourth kinks are generated by the QTM of molecules having, respectively, two and three reversed neighbors. The field shift

between two consecutive kinks is ≈ 0.1 T, corresponding to an interdimer interaction $J' \approx 0.015$ K.

Minor hysteresis loops were measured for different field sweep rates (Fig. 3) and reversal fields (Fig. 4) in order to probe the step heights of the fine structure: the smaller the sweep rate, the higher the resulting kink. This dependence is justified by the Landau-Zener model. The main point to note is that heights of two consecutive kinks are correlated. The second kink height is smaller than the first kink height, the third smaller than the second, and so on. This result is in good agreement with our model: in order to have quantum tunneling of molecules with n reversed neighbors, the n neighbors must have previously reversed. Note that the field sweep rates in Fig. 3 are about two orders of magnitude smaller than in Fig. 4. The magnetization therefore relaxes nearly to equilibrium in Fig. 3, whereas this is not so in Fig.

4, leading to a different relaxation behavior for the back sweeps.

All the other transitions exhibit the same kind of fine structure, which can be explained by the above model leading to the eight combs in Fig. 2(b), giving for the three fitting parameters $D/k_B \approx -0.75$ K, $J/k_B \approx 0.1$ K, and $J'/k_B \approx 0.015$ K.

The above results demonstrate that a three-dimensional network of exchange-coupled SMM's does not suppress QTM. The intermolecular interactions are strong enough to cause a clear field bias, but too weak to transform the spin network into a *classical* antiferromagnetic material. This three-dimensional network of exchange-coupled SMM's demonstrate that the QTM can be controlled using exchange interactions, and opens up new perspectives in the use of supramolecular chemistry to modulate the quantum physics of these molecular nanomagnets.

-
- ¹G. Christou, D. Gatteschi, D.N. Hendrickson, and R. Sessoli, *MRS Bull.* **25**, 66 (2000).
- ²R. Sessoli, H.-L. Tsai, A.R. Schake, S. Wang, J.B. Vincent, K. Folting, D. Gatteschi, G. Christou, and D.N. Hendrickson, *J. Am. Chem. Soc.* **115**, 1804 (1993).
- ³R. Sessoli, D. Gatteschi, A. Caneschi, and M.A. Novak, *Nature (London)* **365**, 141 (1993).
- ⁴S.M.J. Aubin *et al.*, *J. Am. Chem. Soc.* **118**, 7746 (1996).
- ⁵C. Boskovic *et al.*, *J. Am. Chem. Soc.* **124**, 3725 (2002).
- ⁶J.R. Friedman, M.P. Sarachik, J. Tejada, and R. Ziolo, *Phys. Rev. Lett.* **76**, 3830 (1996).
- ⁷L. Thomas, F. Lioni, R. Ballou, D. Gatteschi, R. Sessoli, and B. Barbara, *Nature (London)* **383**, 145 (1996).
- ⁸C. Sangregorio, T. Ohm, C. Paulsen, R. Sessoli, and D. Gatteschi, *Phys. Rev. Lett.* **78**, 4645 (1997).
- ⁹S.M.J. Aubin, N.R. Dilley, M.B. Wemple, G. Christou, and D.N. Hendrickson, *J. Am. Chem. Soc.* **120**, 839 (1998).
- ¹⁰S.M.J. Aubin, N.R. Dilley, M.B. Wemple, G. Christou, and D.N. Hendrickson, *J. Am. Chem. Soc.* **120**, 4991 (1998).
- ¹¹W. Wernsdorfer and R. Sessoli, *Science* **284**, 133 (1999).
- ¹²W. Wernsdorfer, N. Aliaga-Alcalde, D.N. Hendrickson, and G. Christou, *Nature (London)* **416**, 406 (2002).
- ¹³D.N. Hendrickson *et al.*, *J. Am. Chem. Soc.* **114**, 2455 (1992).
- ¹⁴N. Aliaga-Alcalde *et al.* (unpublished).
- ¹⁵W. Wernsdorfer, *Adv. Chem. Phys.* **118**, 99 (2001).
- ¹⁶W. Wernsdorfer, S. Bhaduri, R. Tiron, D.N. Hendrickson, and G. Christou, *Phys. Rev. Lett.* **89**, 197201 (2002).
- ¹⁷These differences cannot be due to differences in the dipole couplings in compounds 1 and 2. We checked and estimated that the dipole coupling between Mn_4 molecules is one order of magnitude smaller than the exchange interaction. In addition, the dipole coupling is similar in both compounds because the structure and unit-cell parameters are nearly identical.